

Radial Stellar Pulsations

Up to this point, you have studied stars in hydrostatic equilibrium. In the next few lectures, we will consider oscillating stars. We begin with the simplest but perhaps most important case: radial pulsators. These stars remain spherically symmetric, though not hydrostatic.¹

Two important classes of radial pulsators are RR Lyrae and delta Cepheid variables. (The term “variable” can be applied to any star whose brightness varies. In addition to various types of pulsators, these include eclipsing binaries, novae, and other stars whose brightness variations have nothing to do with pulsation.) RR Lyraes and Cepheids are important because they are used as distance estimators. These stars are bright and can be recognized at great distances. Furthermore, their periods are closely related to their luminosities. Hence by measuring the period we know the absolute magnitude of such a star, and by comparing this with the apparent magnitude, we deduce the distance.

Delta Cepheids are evolved stars with masses $5-10M_{\odot}$, usually in the helium-core-burning phase. They belong to Population I and are found in the disks of spiral galaxies. (There are other sorts of Cepheid variables, for example beta Cepheids. The delta Cepheids are the brightest and most useful, however, so one usually calls them simply “Cepheids,” or sometimes “classical Cepheids.”) Their absolute visual magnitudes are $M_V = -1$ to -6 (compare the Sun: $M_{V,\odot} = +4.83$). The period-luminosity relation for Cepheids was discovered by Henrietta Leavitt in 1906 ([4]), and it has played an important role in the Galactic and extragalactic distance scale ever since. A recent determination is

$$M_V = -2.88(\pm 0.20) \log\left(\frac{\Pi}{10\text{d}}\right) - 4.12(\pm 0.09)[\pm 0.29], \quad (1)$$

where Π is the period, and the final $[\pm 0.29]$ is the scatter around the mean relation. The other \pm numbers are estimated errors in the mean relation itself. This formula has been taken from a review by [5]. The *slope* (the coefficient of $\log \Pi$ above) can be determined from any group of Cepheids at a common but unknown distance (*e.g.* in the LMC) and is therefore relatively uncontroversial. But the *zero-point* (given as -4.12 above) must be determined by calibration against Cepheids whose distance is known, and is still vigorously debated. Cepheids remain crucial part of the distance ladder and hence of the measurement of the Hubble constant.

RR Lyrae stars are old horizontal-branch stars (hence also core helium burning), low metallicity, and masses $\lesssim 1M_{\odot}$. They belong to Population II; they are found in globular clusters and in the Galactic bulge. The horizontal branch is so named because it forms a sequence of roughly constant luminosity in the HR diagram. Therefore RR Lyraes cover a much smaller range of luminosities than Cepheids; typically, $M_V \approx +0.5 \rightarrow +0.2$. They are fainter than the Cepheids, though still much brighter than the Sun. Within their narrow range of magnitudes, however, the RR Lyraes also satisfy a period-luminosity relation.

A Rough Explanation of the Period-Luminosity Relation

Cepheids, RR Lyraes, and many other pulsators are found in a narrow and nearly vertical strip in the HR diagram. Thus the effective temperatures of these stars are closely similar and only weakly dependent on luminosity ($T_{\text{eff}} \approx 6 \pm 1 \times 10^3$ K). We shall see why this is true shortly. Since $L = 4\pi R^2 \sigma T_{\text{eff}}^4$ and $T_{\text{eff}} \sim \text{constant}$,

$$L \propto R^2. \quad (2)$$

The period of the *fundamental radial mode of pulsation*, in which the entire star expands and contracts together, is determined by the mean density:

$$\Pi \sim (G\bar{\rho})^{-1/2} \propto \left(\frac{M}{R^3}\right)^{-1/2}. \quad (3)$$

Eliminating the stellar radius R between these last two equations, one finds

$$\Pi \propto L^{3/4} M^{-1/2}. \quad (4)$$

¹A more detailed treatment of this subject is given in §§38-39 of the textbook [3].

Since the classical Cepheids are post-main-sequence objects, we cannot use the main-sequence mass-luminosity relation to eliminate M in favor of L . Nevertheless, since L is usually a sensitive function of mass, mass is insensitive to luminosity. Thus equation (4) suggests $\Pi \propto L^x$ with $x \leq 3/4$ since $dM/dL > 0$. However, T_{eff} is not strictly constant within the instability strip: it slowly decreases with increasing L . The empirical relation (1) indicates $\Pi \propto L^{0.87 \pm 0.06}$ if one ignores variations in the bolometric correction.

Frequencies of Adiabatic Radial Modes

The radial modes of a star can be likened to standing sound waves in an organ pipe. For our purposes, an organ pipe is a cylinder capped at one end but open at the other. The pressure and velocity perturbations in a standing acoustic wave are 90° out of phase. Thus at the closed end of the pipe, the velocity vanishes and the pressure fluctuations are maximal. Similarly, at the center of a radially pulsating star, the radial velocity has a node and the pressure has an antinode. At the open end of the organ pipe and at the surface of a star, the situation is reversed: the pressure fluctuations vanish and those of the velocity are maximal. (The latter boundary condition is inaccurate for organ pipes, because it doesn't allow for radiation of sound, but is better for stars.) In this approximation, the length of the pipe, a , is one quarter of the wavelength of the fundamental. Thus the lowest note—the fundamental—has period $\Pi_0 = 4a/v_s$. The sound speed of the star varies with radius, and furthermore gravitational forces modify the period, but nevertheless we may expect that

$$\Pi_0 \sim 4 \frac{R}{\bar{v}_s}. \quad (5)$$

The equation of hydrostatic equilibrium,

$$\frac{dP}{dr} = -\frac{GM_r \rho}{r^2}, \quad (6)$$

can be very crudely approximated by

$$\frac{\bar{P}}{R} \sim \frac{GM\bar{\rho}}{R^2}, \quad \text{or} \quad \frac{\bar{P}}{\bar{\rho}} \sim \frac{GM}{R}, \quad (7)$$

where \bar{P} and $\bar{\rho}$ represent the average pressure and the average density in the star. The combination $\bar{P}/\bar{\rho}$ is related to the sound speed, v_s :

$$v_s^2 \equiv \left(\frac{\partial P}{\partial \rho} \right)_s \equiv \Gamma_1 \frac{P}{\rho}. \quad (8)$$

Since the adiabatic index Γ_1 is always of order unity, it follows that

$$\bar{v}_s \sim \left(\frac{GM}{R} \right)^{1/2}. \quad (9)$$

Putting this into eq. (5), we find that the fundamental frequency is of order

$$\Pi_0 \sim 4 \left(\frac{GM}{R^3} \right)^{-1/2}, \quad (10)$$

in agreement with eq. (3). In fact, for an $n = 3/2$ polytrope with $\Gamma_1 = 5/3$, the rough estimate (10) is remarkably accurate: the actual numerical coefficient turns out to be 3.815 instead of 4. For a star having the equilibrium structure of an $n = 3$ polytrope but responding to adiabatic perturbations with $\Gamma_1 = 5/3$ (this is a crude model of the Sun), the coefficient is 2.065 [[1], Table 8.1].

By variational methods akin to Rayleigh-Ritz, which you may have encountered in quantum mechanics, it is possible to establish the following bounds on the angular frequency ($\omega_0 \equiv 2\pi/\Pi_0$) of the fundamental mode:

$$(3\Gamma_1 - 4) \left(\frac{GM}{R^3} \right) \leq \omega_0^2 \leq (3\Gamma_1 - 4) \frac{|W|}{I}, \quad (11)$$

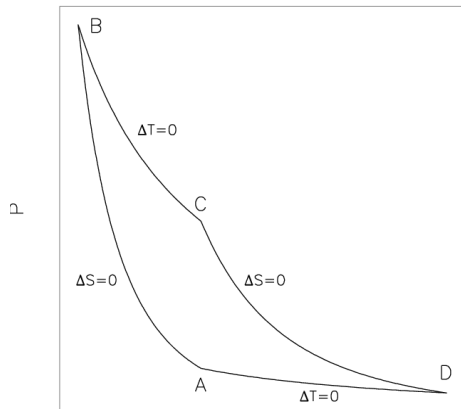


Figure 1: The Carnot cycle.

in which

$$W \equiv - \int \frac{Gm}{r} dm \quad (12)$$

is the gravitational potential energy of the star and

$$\frac{2}{3}I \equiv \frac{2}{3} \int r^2 dm \quad (13)$$

is the moment of inertia. For a derivation, see Chapter 8 of [1]. It is assumed here that pressure and density fluctuations are connected by the adiabatic relation (8) with Γ_1 constant throughout the star. The lefthand inequality in eq. (11) must be reversed if $\Gamma_1 < 4/3$. In this case both limits imply that $\omega^2 < 0$, so that the fundamental mode grows exponentially. Like a white dwarf above the Chandrasekhar mass, such a star is unstable to gravitational collapse.

In an organ pipe, higher harmonics exist in addition to the fundamental, with wavelengths $\lambda_n = 4a/(2n + 1)$ and periods $\Pi_n = \lambda_n/v_s$. Because the sound speed varies with radius in a given star, its pulsational harmonics are not so simply related. However, the periods decrease monotonically with increasing numbers of nodes. The n^{th} overtone has n nodes in the velocity or displacement, not counting the node that is always present at $r = 0$. The ratio Π_1/Π_0 of the period of the first overtone to that of the fundamental measures the degree of central concentration of the star; this ratio tends to increase as the central density increases with respect to the mean density. For example, Π_1/Π_0 is 0.465 and 0.738 for the $(n, \Gamma_1) = (3/2, 5/3)$ and $(3, 5/3)$ polytropes, respectively ([1]).

Excitation of radial pulsations: The Kappa and Epsilon Mechanisms

If the adiabatic approximation were exact, or in other words if the entropy of every gas element were constant through the pulsation cycle, then the energy in pulsations would be conserved. Oscillations of stars with $\Gamma_1 > 4/3$ throughout most of their interior would neither grow nor decay. One might think that nonadiabatic effects, such as viscosity and radiative diffusion, would tend to damp the oscillations. This is indeed usually the case. Under certain circumstances, however, nonadiabatic effects may actually excite pulsations.

To see how this can happen, it is useful to convert our organ pipe of the previous section into a heat engine. Fill the open end with a movable piston and allow the pipe to make thermal contact with hot and cold heat baths. Just to remind you, the classical Carnot engine works as follows (refer to Figure 1):

- $A \rightarrow B$: The piston is compressed adiabatically, that is, at constant entropy: $\Delta S_{AB} = 0$. Pressure P , volume V , and temperature T vary as $P \propto V^{-\Gamma_1}$ and $T \propto V^{1-\Gamma_1}$. The temperature increases from T_A to $T_B = T_A(V_A/V_B)^{\Gamma_1-1}$.
- $B \rightarrow C$: The gas is brought into contact with the hotter heat bath, $T_{\text{hot}} = T_B$, and allowed to expand at constant temperature. Since $PV \propto T$ and T is constant, $P \propto V^{-1}$. During this step, the entropy increases by $\Delta S_{BC} = \Delta Q_{BC}/T_{\text{hot}}$, where ΔQ_{BC} is the heat added to the gas.
- $C \rightarrow D$: The gas is detached from the heat bath and allowed to expand adiabatically until its temperature falls back to $T_A = T_{\text{cold}}$. At this point the volume is larger than V_A because of the increase in entropy during the previous step.
- $D \rightarrow A$: Finally, the gas is brought into contact with the cold bath at temperature T_{cold} and isothermally recompressed to its original volume V_A . In this step, $\Delta S_{DA} = \Delta Q_{DA}/T_{\text{cold}}$. Since S (a function of state) must return to its original value, $\Delta S_{DA} = -\Delta S_{BC}$. So $\Delta Q_{BC} + \Delta Q_{DA} = \Delta Q_{BC}(T_{\text{hot}} - T_{\text{cold}})/T_{\text{hot}} > 0$. Thus net heat is absorbed by the engine, and energy conservation requires that the heat is converted to work.

The net work done by the gas on the piston is

$$\Delta W = \oint_{ABCD A} P dV, \quad (14)$$

which is the area enclosed by the curve in the (V, P) plane. Since the internal energy (U) returns to its original value after one complete cycle, $\oint dU = 0$. Therefore using the First Law, $dU = TdS - PdV$, we can rewrite the work done as

$$\Delta W = \oint T dS. \quad (15)$$

Clearly $\Delta W > 0$ along any clockwise closed path, not just those composed of adiabats and isotherms. Hence if the gas tends to gain entropy when it is compressed (at high temperature) and to lose it when expanded (at lower temperature), then the net work done is positive.

In the Carnot engine described above, heat and entropy are gained or lost only when the gas is in contact with a heat bath. At the center of a star, however, heat and entropy are continually produced by nuclear reactions. In equilibrium, heat production in the core is exactly balanced by heat loss from the surface, *i.e.*, by the stellar luminosity. Stellar pulsation disturbs this balance by

- (i) modulating the nuclear reaction rate in the core (*epsilon mechanism*); and more importantly,
- (ii) by modulating the radiative luminosity (*kappa mechanism*).

Effect (i) is always destabilizing because the nuclear reaction rate increases with increasing temperature and pressure: thus the change in reaction rate tends to add entropy to the core when it is at higher than equilibrium temperature. Except in very massive stars ($\gtrsim 100 M_{\odot}$), the epsilon mechanism tends to be weak, so that a small amount of dissipation is enough to prevent growth.

At the lower temperatures characteristic of the outer envelopes of stars, the opacity may actually increase with temperature (at fixed entropy, for example) because the gas is incompletely ionized. In such a case, luminosity decreases when the star contracts and its temperature rises, trapping heat in the interior and raising the entropy; the reverse is true when the star expands. During one period of oscillation, most mass shells then execute a clockwise closed path in the (S, T) and (V, P) planes, leading to an increase in mechanical energy.

The reason for the increase of opacity with temperature is roughly as follows. In the solar photosphere, almost all of the hydrogen atoms are in their ground state ($n = 1$). To excite such an atom into the higher states requires photons energies of ≥ 10.2 eV, whereas the characteristic photon energy at 5700 K is only $kT = 0.49$ eV. Hence neutral hydrogen contributes little to the opacity, which is in fact dominated by the weakly bound H^- ion. At modestly higher temperatures $\sim 10^4$ K, a small but significant proportion of the hydrogen lies in excited states, where the spacing

between adjacent levels is smaller ($\propto n^{-3}$), as is the ionization energy ($\propto n^{-2}$), so that the opacity is dominated by the excited neutral hydrogen. At these temperatures, $\partial\kappa/\partial T > 0$. At still higher temperatures, the fraction of the hydrogen in excited bound states actually decreases with increasing temperature because most of the hydrogen is already ionized; since free electrons are much less effective than bound ones at absorbing photons, the hydrogen opacity then decreases with further increases in T . However, at $T \sim 4 \times 10^4$ K, helium is in transition between singly and doubly ionized states and tends to cause $\partial\kappa/\partial T > 0$.

These opacity effects constitute the kappa mechanism (ii). We can understand the physics in a bit more detail by returning to the work integral in the form (15). The gas within the Carnot engine is uniform in temperature, so S represents the total entropy of this gas. In the case of a star, since the temperature varies with radius, we must evaluate TdS separately for each mass shell; hence $S(m, t)$ becomes the entropy per unit mass at mass fraction m (this notation will be used in place of M_r in this lecture), and

$$\Delta W = \int_{t'}^{t'+\Pi} dt \int_0^M dm T \frac{dS}{dt}. \quad (16)$$

Replace $T(m, t) \rightarrow \bar{T}(m) + \delta T(m, t)$ and $S(m, t) \rightarrow \bar{S}(m) + \delta S(m, t)$, where $\bar{T}(m)$ and $\bar{S}(m)$ are the time-averaged temperature and entropy of the shell, and δT and δS have zero time average. Then the work integral becomes

$$\Delta W = \oint dt \int dm \delta T \frac{d\delta S}{dt}. \quad (17)$$

The limits of integration are the same as before but will not be written out explicitly. Notice that this is second order in the oscillating quantities; the zeroth-order terms vanish because $d\bar{S}/dt = 0$, and the first-order terms vanish in the time average:

$$\left\langle \bar{T} \frac{d\delta S}{dt} \right\rangle = \bar{T} \left\langle \frac{d\delta S}{dt} \right\rangle = 0.$$

In the fundamental radial mode, the entire star expands and contracts together. Hence the sign of δT is independent of mass fraction, and since the pulsation is approximately homologous—*i.e.*, the fractional change in radius $\delta r/r$ and volume $\delta V/V$ is approximately the same for most mass shells—even the magnitude of $\frac{\delta T}{T}$ is approximately constant with mass fraction. Thus it is useful to pull the fractional temperature perturbation out of the mass integral:

$$\Delta W \approx \oint dt \left\langle \frac{\delta T}{\bar{T}} \right\rangle_m \int dm \bar{T} \frac{d\delta S}{dt}, \quad (18)$$

where the angle brackets indicate an appropriate average over mass at time t . Finally, if we ignore changes in the nuclear reaction rate, then to first order,

$$\bar{T} \frac{d\delta S}{dt} \approx -\frac{\partial \delta L}{\partial m}(m, t). \quad (19)$$

The mass integral in eq. (18) now yields $\delta L(r, M) - \delta L(r, 0)$, and this = $\delta L(r, M)$ since $L(r, 0) = 0$ even under perturbation. Writing $\delta L(t) \equiv \delta L(M, t)$ for the change in the total stellar luminosity, we have at last

$$\Delta W \approx - \oint dt \left\langle \frac{\delta T}{\bar{T}} \right\rangle_m \delta L(t). \quad (20)$$

The luminosity, opacity, and temperature are related by

$$L(m, t) = -16\pi^2 r^4 \frac{c}{\kappa} \frac{\partial P_{\text{rad}}}{\partial m}, \quad (21)$$

where $P_{\text{rad}} = \frac{1}{3}aT^4$. At sufficient depth below the photosphere, we may evaluate δL from this equation using the adiabatic values for δT , $\delta\rho$, and δr . Variations in opacity, radius, and radiative gradient contribute additively to first order. Clearly if

$$\left(\frac{\partial\kappa}{\partial T}\right)_S = \left(\frac{\partial\kappa}{\partial T}\right)_\rho + \left(\frac{\partial\kappa}{\partial\rho}\right)_T \left(\frac{\partial\rho}{\partial T}\right)_S > 0,$$

then the opacity will increase during contractions. The second term on the righthand side tends to be positive since $(\partial\kappa/\partial\rho)_T \geq 0$ and $(\partial\rho/\partial T)_S > 0$. The first can be positive at low temperatures: see Figure 17.5 in the textbook [3]. This will tend to make the product $\delta L\delta T < 0$ in eq. (20). The decrease in radius during contractions reinforces this tendency because of the r^4 factor in eq. (21). On the other hand, $\delta P_{\text{rad}} > 0$ in contractions and this implies $\partial\delta P_{\text{rad}}/\partial m < 0$ in a homologous contraction:

$$\frac{\partial}{\partial m}\delta P_{\text{rad}} = \frac{\delta P_{\text{rad}}}{P_{\text{rad}}}\frac{\partial P_{\text{rad}}}{\partial m}.$$

So the first two effects must be stronger than the last in order to guarantee that $\Delta W > 0$, *i.e.*, in order to increase the mechanical energy of the pulsation.

In the argument above, we evaluated the change in luminosity using the *adiabatic* variations in T , r , and ρ . This is only an approximation, since it is precisely the deviation from adiabatic behavior that makes growth possible. The approximation is valid if the local thermal timescale of the ionization zone (*i.e.* the region where $\partial\kappa/\partial T > 0$) is long compared to the pulsation period. The local thermal timescale may be defined as the thermal energy of the matter exterior to the base of the ionization zone, divided by the luminosity:

$$t_{\text{therm}} \sim (M - m) \frac{P}{\rho L} \Big|_{m=m_{\text{ioniz}}}. \quad (22)$$

If $t_{\text{therm}} \ll \Pi$, then the adiabatic approximation fails completely in the ionization zone: the radiative gradient will quickly compensate for any change in opacity so that the luminosity is not affected by the pulsation and $\Delta W \approx 0$. As T_{eff} increases, the ionization zones move closer to the surface and t_{therm} decreases, and at some point the instability is quenched. This determines the blue, *i.e.* high- T_{eff} , edge of the “instability strip” in the HR diagram where Cepheids occur. On the other hand, if the ionization zone lies too far below the surface, then $t_{\text{therm}} \gg \Pi$ both in the ionization zone and in the regions immediately above it; modulation of the local luminosity in the ionization zone then has little effect on $\delta L(t)$ emerging from the surface, which is determined by local conditions in some shallower zone where $t_{\text{therm}} \approx \Pi$. Furthermore, as T_{eff} decreases and the ionization zones retreat to greater depths, they become convective, at which point the opacity no longer controls the radiative flux. These effects determine the red edge of the instability strip.

Our derivation of the kappa mechanism is impressionistic rather than rigorous. The proper way to determine pulsational stability is to linearize the full non-steady stellar structure equations and solve for the complex eigenfrequencies directly. This is described in [1] and will not be repeated here.

Direct Determination of Distance: The Baade-Wesselink Method

We have noted that once a period-luminosity relation has been established, pulsating stars can serve as distance indicators. Remarkably, however, the distance to a pulsating star can be determined directly, in principle, without prior knowledge of the PL relation.

The flux received from a star of radius R , distance D , and effective temperature T_{eff} is

$$F = \frac{R^2\sigma T_{\text{eff}}^4}{D^2}. \quad (23)$$

The flux and effective temperature of a pulsating star vary with time, but these are directly measurable if we have photometry in multiple filters, or better yet series of spectra. Taking the log of eq. (23) and differentiating, one has

$$\frac{d}{dt} \ln F = 4 \frac{d}{dt} \ln T_{\text{eff}} + \frac{2}{R} \frac{dR}{dt}. \quad (24)$$

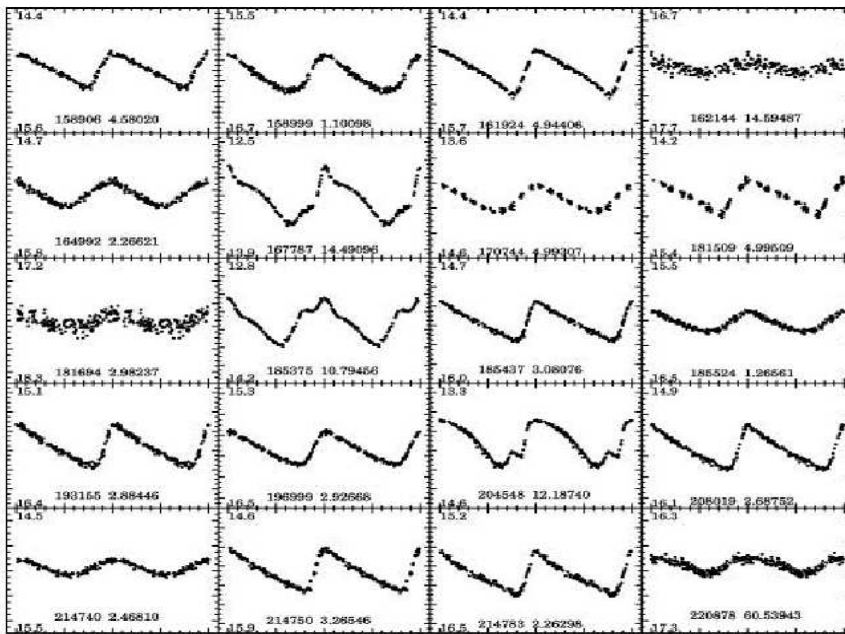


Figure 2: Light curves of a few of the LMC Cepheids found by the OGLE II project [7].

Notice that the distance has dropped out because it is constant. One can solve the above for the stellar radius in terms of measurable quantities:

$$R = 2 \frac{dR}{dt} \left(\frac{d}{dt} \ln F - 4 \frac{d}{dt} \ln T_{\text{eff}} \right)^{-1}. \quad (25)$$

Here dR/dt is measured by the doppler shift of stellar absorption or emission lines. Once R is known, eq. (23) can be solved for D . An obvious consistency check is that the derived distance should not vary over the pulsation cycle.

This elegant method suffers some practical difficulties. First, determining T_{eff} from colors or spectra is not trivial. The star does not radiate as a blackbody—if it did, there would be no spectral lines with which to measure the radial velocity. Second, the spectral lines used for the velocity and the continuum represented by T_{eff} are not formed at quite the same radius. This means of course that the lines and the continuum may have different velocities. Both difficulties can be conquered in principle by detailed physical modeling of the moving stellar atmosphere, but this is computationally challenging. The field is still under development.

Incidentally, eq. (25) does not require that the pulsation be periodic. The same technique has been used to measure distances to extragalactic Type II supernovae, but this application is called by its practitioners “The Expanding Photosphere Method” [[6], [2]].

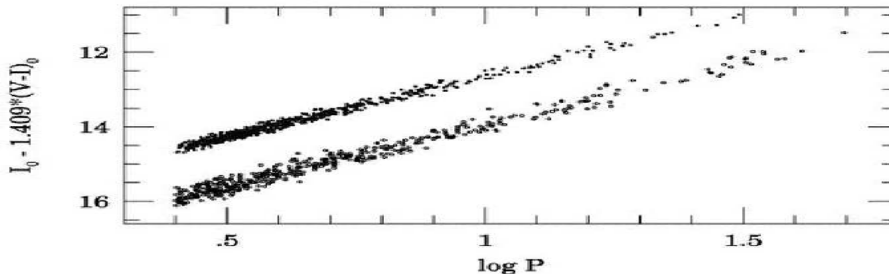


Figure 3: I-band period-luminosity relation of the fundamental-mode Cepheids in the LMC (upper points) and SMC (points shifted down by 0.8 mag) [8].

Calculation of linear adiabatic radial pulsations

To determine the pulsational eigenmodes of a given stellar model, one starts with the full radial force equation in the form

$$\left(\frac{\partial^2 r}{\partial t^2}\right)_m = -4\pi r^2 \left(\frac{\partial P}{\partial m} + \frac{Gm}{4\pi r^4}\right). \quad (26)$$

There is an equilibrium state in which $r(m, t) = r_0(m)$ and both sides of the equation vanish. Define $\delta r(m, t) \equiv r(m, t) - r_0(m)$, and similarly $\delta P(m, t)$, $\delta \rho(m, t)$, *etc.* Presuming that these perturbations are small, expand (26) to first order, obtaining

$$\delta \ddot{r} = -4\pi r^2 \left(\frac{\partial \delta P}{\partial m} - 4\frac{Gm}{4\pi r^5} \delta r\right).$$

The following equations are slightly tidier if r_0 rather than m is used as independent variable. To save writing, the subscript will be omitted from r_0 , but it should be remembered that unless prefixed by δ , r will refer to the *equilibrium* radius of a given mass shell. Then the last equation becomes

$$\delta \ddot{r} = -\frac{1}{\rho} \frac{\partial \delta P}{\partial r} + 4\frac{GM_r}{r^3} \delta r. \quad (27)$$

We have put $m \rightarrow M_r$ to remind ourselves that it refers to the mass contained within the equilibrium radius r . The dots refer to derivatives with respect to t at constant m or r_0 .

As yet, we have not used the assumption of adiabaticity, but we are about to do so:

$$\delta P = \left(\frac{\partial P}{\partial \rho}\right)_S \delta \rho = \Gamma_1 P \frac{\delta \rho}{\rho}, \quad \text{where} \quad \Gamma_1 \equiv \left(\frac{\partial \ln P}{\partial \ln \rho}\right)_S. \quad (28)$$

In a gas-pressure-dominated star, $\Gamma_1 \approx 5/3$ everywhere—in radiative as well as convective regions—because Γ_1 describes not the equilibrium (in which entropy may vary with radius) but the response of a given mass element to adiabatic perturbations. Conservation of mass implies

$$\frac{\delta \rho}{\rho} = -\frac{1}{r^2} \frac{\partial}{\partial r} (r^2 \delta r). \quad (29)$$

By combining (28) and (29), one converts (27) to an equation involving δr alone:

$$\delta \ddot{r} = \frac{1}{\rho} \frac{\partial}{\partial r} \left[\frac{\Gamma_1 P}{r^2} \frac{\partial}{\partial r} (r^2 \delta r) \right] + 4 \frac{GM_r}{r^3} \delta r. \quad (30)$$

For an eigenmode, all mass shells should vibrate at the same frequency: that is,

$$\begin{aligned} \delta r(m, t) &= \xi(r) e^{-i\omega t}, \quad \text{so that} \\ -\omega^2 \xi &= \frac{1}{\rho} \frac{d}{dr} \left[\frac{\Gamma_1 P}{r^2} \frac{d}{dr} (r^2 \xi) \right] + 4 \frac{GM_r}{r^3} \xi. \end{aligned} \quad (31)$$

For numerical work, it is often convenient to unpack (31) as a pair of ordinary differential equations by introducing $\eta \equiv r^{-2} d(r^2 \xi)/dr$, which is essentially just $-\delta\rho/\rho$, so that

$$\begin{aligned} \frac{d\xi}{dr} &= \eta - \frac{2}{r} \xi, \\ \frac{1}{\rho} \frac{d}{dr} (\Gamma_1 P \eta) &= -\omega^2 \xi - \frac{4GM_r}{r^3} \xi. \end{aligned} \quad (32)$$

The boundary condition at $r = 0$ is obviously $\xi = \delta r = 0$. The boundary condition at $r = R$ (the equilibrium outer radius) is not so obvious, but it can be obtained from the requirement that ξ should be regular as $r \rightarrow R$: that is, $\xi(r)$ and at least its first few derivatives with respect to r should exist at $r = R$. [In fact, the requirement of regularity as $r \rightarrow 0$ gives the central b.c., $\xi(0) = 0$, as can be seen from the first of equations (32).] Let us rewrite the second of equations (32) in the form

$$\frac{\Gamma_1 P}{\rho} \frac{d\eta}{dr} - \Gamma_1 \frac{GM_r}{r^2} \eta = - \left(\omega^2 + \frac{4GM_r}{r^3} \right) \xi. \quad (33)$$

The coefficient of $d\eta/dr$ in this equation is v_s^2 , which is proportional to temperature for an ideal gas and therefore very small at the surface compared to its value at the center. In fact, for the purpose of computing modes of oscillation, one often approximates the hydrostatic equilibrium structure by models in which $v_s^2 \rightarrow 0$ as $r \rightarrow R$. If the solution is to be regular, then $d\eta/dr$ will be finite as $r \rightarrow R$; in fact $d\eta/dr \sim \xi/R^2$ there. So the first term on the lefthand side of (33) essentially vanishes at $r = R$, and the boundary conditions become

$$\eta = -\frac{1}{\Gamma_1 R} \left(\frac{R^3 \omega^2}{GM} + 4 \right) \xi \quad \text{at } r = R \quad (34)$$

$$\xi = 0 \quad \text{at } r = 0. \quad (35)$$

The surface boundary condition (34) is only approximate and would break down for high-frequency modes whose wavelength is shorter than the pressure scale height at the photosphere; in the Sun, this occurs for $\Pi \lesssim 3$ min, whereas $\Pi_{0,\odot} \sim 1$ hr.

We may solve equations (32), (34) & (35) by shooting to a fitting point, *i.e.* integrating outward from $r = 0$ and inward from $r = R$ to an intermediate radius r_{fit} . But we have *three* unknowns to guess: $\eta(0)$, $\xi(R)$, and ω itself. Fortunately, because the differential equations are linear and homogeneous, we do not have to solve for all three simultaneously. We can freely rescale the dependent variables by a common factor—and we may choose these scaling factors independently for the inward and outward integrations to minimize the mismatch at r_{fit} . This freedom reduces the number of matching conditions from two to one:

$$\begin{bmatrix} \eta \\ \xi \end{bmatrix}_{\text{outward}} = \begin{bmatrix} \eta \\ \xi \end{bmatrix}_{\text{inward}} \quad \text{at } r = r_{\text{fit}}. \quad (36)$$

Since both sides of this equation are independent of the scaling factors, we may choose $\eta(0)$ and $\xi(R)$ arbitrarily—I generally just set both to unity. Then we have a one-dimensional search over ω^2 to perform in order to satisfy (36). The lowest root for ω^2 is the fundamental mode. After finding ω , we may easily rescale $\eta(0)$ and $\xi(R)$ so as to obtain continuous solutions for ξ and η .

References

- [1] J. P. Cox. *Theory of Stellar Pulsation*. Princeton University Press, 1980.
- [2] R. G. Eastman, B. P. Schmidt, and R. Kirshner. The Atmospheres of Type II Supernovae and the Expanding Photosphere Method. *ApJ*, 466:911–937, August 1996.
- [3] R. Kippenhahn and A. Weigert. *Stellar Structure and Evolution*. Springer, 1990.
- [4] H. Leavitt. 1777 Variables in the Magellanic Clouds. *Ann. Harvard Coll. Obs.*, 60(4), 1908.
- [5] B. F. Madore and W. L. Freedman. The Cepheid distance scale. *PASP*, 103:933–957, September 1991.
- [6] B. P. Schmidt, R. P. Kirshner, and R. G. Eastman. Expanding photospheres of type II supernovae and the extragalactic distance scale. *ApJ*, 395:366–386, August 1992.
- [7] A. Udalski, I. Soszynski, M. Szymanski, M. Kubiak, G. Pietrzynski, P. Wozniak, and K. Zebrun. The Optical Gravitational Lensing Experiment. Cepheids in the Magellanic Clouds. IV. Catalog of Cepheids from the Large Magellanic Cloud. *Acta Astronomica*, 49:223–317, September 1999.
- [8] A. Udalski, M. Szymanski, M. Kubiak, G. Pietrzynski, I. Soszynski, P. Wozniak, and K. Zebrun. The Optical Gravitational Lensing Experiment. Cepheids in the Magellanic Clouds. III. Period-Luminosity-Color and Period-Luminosity Relations of Classical Cepheids. *Acta Astronomica*, 49:201–221, September 1999.